IOP Publishing New J. Phys. 26 (2024) 055002 https://doi.org/10.1088/1367-2630/ad48ac

New Journal of Physics
The open access journal at the forefront of physics

Deutsche Physikalische Gesellschaft DPG
IOP Institute of Physics

Published in partnership with: Deutsche Physikalische Gesellschaft and the Institute of Physics

OPEN ACCESS

RECEIVED
27 February 2024

REVISED
16 April 2024

ACCEPTED FOR PUBLICATION
8 May 2024

PUBLISHED
21 May 2024

PAPER

DarkGEO: a large-scale laser-interferometric axion detector

Joscha Heinze[1,*], Alex Gill[1], Artemiy Dmitriev[1], Jiří Smetana[1], Tianliang Yan[1], Vincent Boyer[1], Denis Martynov[1], Hartmut Grote[2], James Lough[3], Aldo Ejlli[3] and Guido Müller[3]

[1] University of Birmingham, School of Physics and Astronomy, Birmingham B15 2TT, United Kingdom
[2] Cardiff University, School of Physics and Astronomy, Cardiff CF24 3AA, United Kingdom
[3] Max Planck Institute for Gravitational Physics (Albert Einstein Insitute), Hanover 30167, Germany
[*] Author to whom any correspondence should be addressed.

E-mail: j.heinze@bham.ac.uk

Keywords: dark matter, axions, axion-like particles, quantum-enhanced laser interferometry

Abstract

Axions and axion-like particles (ALPs) are leading candidates for dark matter. They are well motivated in many extensions of the standard model and supported by astronomical observations. We propose an iterative transformation of the existing facilities of the gravitational-wave detector and technology testbed GEO600, located near Ruthe in Germany, into a kilometre-scale upgrade of the laser-interferometric axion detector LIDA. The final DarkGEO detector could search for coincident signatures of axions and ALPs and significantly surpass the current constraints of both direct searches and astrophysical observations in the measurement band from 10^{-16} to 10^{-8}eV. We discuss design parameters and sensitivities for the configurations of the different iteration steps as well as technical challenges known from the first LIDA results. The proposed DarkGEO detector will be well suited to probe the mass-coupling parameter space associated with predictions from theoretical models, like grand-unified theories, as well as from astrophysical evidence, like the cosmic infrared background.

1. Introduction

A wealth of evidence from astronomical observations indicates the existence of dark matter and, for several decades, weakly interacting massive particles (WIMPs) were the most prominent candidate for it. A variety of observatories have, however, not been able to detect any WIMP [1–3] and, meanwhile, another candidate has arisen in the dark matter research focus: axions and axion-like particles (ALPs) [4–6]. While the axion is specifically known since 1977 as a solution to the strong charge-parity problem in quantum-chromodynamics [7–10], both types of particle emerge generically in a plentitude of extensions of the standard model, e.g. from string theory and supergravity [11–15]. Furthermore, there are compelling observations from gravitational lensing which distinctly favour wave-like dark matter and which the axion could explain [16].

This gain in significance has led to the proposal of numerous methods and experiments to directly measure the signature of an axion or ALP, some of which have already taken data. Among those are axion haloscopes (ADMX [17], MADMAX [18] and DMRadio [19]), axion helioscopes (CAST [20] and IAXO [21]), 'light shining though a wall' experiments (ALPS [22] and CROWS [23]) and magnetometers (ABRACADABRA [24]). This article considers a fairly new type of direct axion detector based on laser interferometry. This type was proposed in [25–30], and first engineering and observing runs have been conducted in [31] (LIDA) and [32] (DANCE).

The most important component of these detectors is an optical travelling-wave cavity which has a geometrical length of 5 m in LIDA and 45 cm in DANCE. Similarly to the laser-interferometric gravitational-wave detectors [33–35], a kilometre-scale cavity would, however, allow for a significant increase in the sensitivity due to an increased interaction time between the laser field and the axion field and due to additional benefits that, for instance, come with larger mirrors and, thus, larger beam sizes.

In this article, we discuss how the gravitational-wave detector and technology testbed GEO600, located near Ruthe in Germany, could iteratively be tranformed into the next-generation LIDA upgrade 'DarkGEO', featuring a total of two 600 m long cavities for coincidence searches with an additional drastic increase in the operating laser power. Section 2 briefly explains the signal generation in such a laser-interferometric axion detector, in general, and section 3 describes the three main configurations of DarkGEO which can be operated during its iterative transformation, including their design parameters and sensitivities. Finally, section 4 discusses some technical challenges which are known from the first LIDA results and proposes viable solutions for them.

2. Theory

The laser-interferometric axion detectors can measure a signature due to the interaction of the axions with the photons of a laser field. This interaction is governed by the following Lagrangian term [20]

$$\mathcal{L}_{a\gamma} = -\frac{g_{a\gamma}}{4} a F^{\mu\nu} \tilde{F}_{\mu\nu} \,, \tag{1}$$

where a is the axion field, F is the electro-magnetic field-strength tensor and $g_{a\gamma}$ is the axion-photon coupling coefficient. Here, an axion with mass m_a behaves like a coherent classical field [36]

$$a(t) = a_0 \sin\left[\Omega_a t + \delta(t)\right] \tag{2}$$

with angular frequency $\Omega_a = 2\pi f_a = m_a c^2/\hbar$, field amplitude $a_0^2 = 2\rho_{\mathrm{DM}}\hbar^2/m_a^2$, the local density of dark matter $\rho_{\mathrm{DM}} \approx 5.3 \times 10^{-22}\,\mathrm{kg\,m^{-3}}$ [37], and the phase of the field $\delta(t)$.

The measurable effect of the interaction between a linearly polarised 'main' laser field and this axion field is a periodic rotation of the main laser field's polarisation axis. This rotation results from a phase $\Delta\phi$ which accumulates between the left- and right-handed circular states of polarisation over a time period of τ (which will later be the light's cavity roundtrip time) [25]

$$\Delta\phi(t,\tau) = g_{a\gamma}\left[a(t) - a(t-\tau)\right] \,. \tag{3}$$

The periodic rotation of the polarisation axis can be equivalently understood as the excitation of two coherent 'sidebands' which are linearly polarised in the direction orthogonal to the main laser field's polarisation. These two sidebands comprise the signal field and are shifted in frequency by $\pm\Omega_a$ relative to the main laser field. If this effect occurs in an optical cavity that is kept on resonance with the main laser field, these sidebands build up according to [25]

$$\begin{aligned} E_{\mathrm{sig,cav}}(\pm\Omega_a) = &-\frac{E_{\mathrm{m,cav}} \exp\left(i\frac{\beta \mp \Omega_a\tau}{2} + \delta\right)}{1 - \sqrt{1 - 2T_{\mathrm{sig}} - l_{\mathrm{rt}}}\exp\left[i(\beta \mp \Omega_a\tau)\right]} \\ &\times g_{a\gamma}\frac{\tau}{4}\mathrm{sinc}\left(\frac{\Omega_a\tau}{4}\right)\cos\left(\frac{2\beta \mp \Omega_a\tau}{4}\right)\sqrt{2\tau_a\rho_{\mathrm{DM}}} \,. \end{aligned} \tag{4}$$

$E_{\mathrm{m,cav}}$ is the circulating intra-cavity main field, β takes into account that the cavity resonances for the polarisations of the main and signal field may be non-degenerate in frequency, τ is the cavity roundtrip time, T_{sig} is the power transmissivity of the cavity input and output couplers for the signal field polarisation, l_{rt} is the cavity roundtrip power loss and τ_a is the coherence time of the axion field.

In either transmission or reflection of the cavity, the signal field can be superimposed with a strong coherent local oscillator field E_{LO} by shifting a constant fraction of the main field into the signal polarisation via a half-wave plate. The amplitude spectral density P_{out} of the signal is then obtained from the beatnote between the local oscillator and the sidebands [25]:

$$P_{\mathrm{out}}(\Omega_a) = E_{\mathrm{LO}}\sqrt{T_{\mathrm{sig}}}\left[E^*_{\mathrm{sig,cav}}(-\Omega_a) - E_{\mathrm{sig,cav}}(\Omega_a)\right] \,. \tag{5}$$

Here, $i\sqrt{T_{\mathrm{sig}}}E^{(*)}_{\mathrm{sig,cav}}(\pm\Omega_a)$ are the two signal sidebands after being coupled out of the cavity in transmission or reflection. The signal-to-noise-ratio finally depends on the amplitude spectral density of the total noise P_N at the signal frequency Ω_a and on the total measurement time T_{meas}:

$$\mathrm{SNR}^2 = \left|\frac{P_{\mathrm{out}}(\Omega_a)}{P_{\mathrm{N}}(\Omega_a)}\right|^2 \sqrt{\frac{T_{\mathrm{meas}}}{\tau_a}} \,. \tag{6}$$

For a thorough theoretical description of the operating principle, we refer to [25–30].

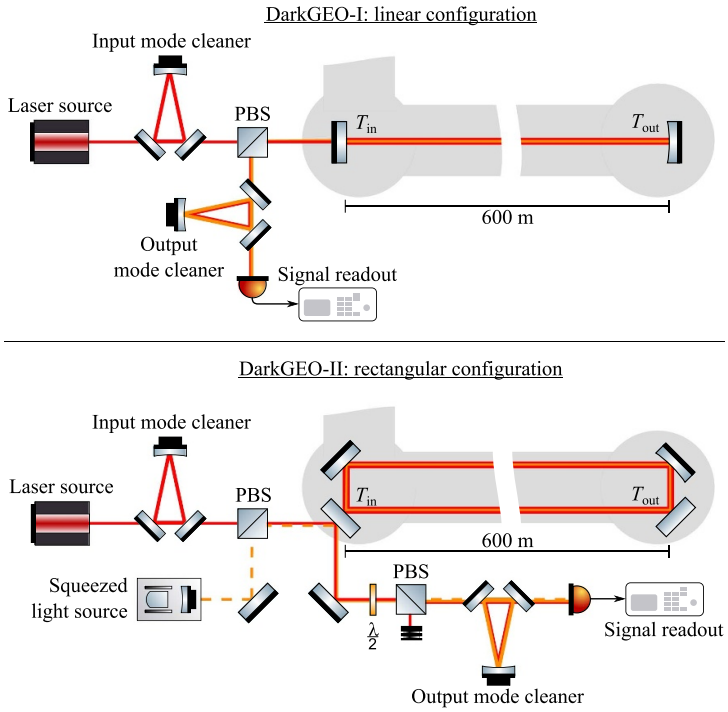

Figure 1. Simplified schematic of the DarkGEO-I and -II configurations with one linear and one rectangular cavity, respectively. PBS: polarising beamsplitter, red beam: main laser field, orange beam: signal field, dashed beam: squeezed field. The second arm of the GEO600 facility is indicated as going upwards.

3. Design

The GEO600 facilities are constructed to house a laser-interferometric gravitational-wave detector in the typical Michelson topology [38]. Most importantly, the facilities provide two 600 m long vacuum tubes whose end stations are equipped with mirror suspension platforms for vibrational isolation as well as with optical tables.

3.1. DarkGEO-I: linear configuration

The first iteration step of the proposed DarkGEO detector only requires minor changes to the GEO600 design and is similar to the proposal in [30]. Instead of using a rectangular travelling-wave cavity as in LIDA and DANCE, DarkGEO-I consists of one linear standing-wave cavity that is set up with a length of 600 m in one of the vacuum tubes between the current positions of the beamsplitter and the far end stage. This is shown in the top schematic of figure 1.

A linear cavity only offers a limited broadband sensitivity to axions and axion-like particles because the reflection off a mirror under normal incidence causes a phase shift of π between the main laser field (here, vertical polarisation) and signal field (here, horizontal polarisation). Hence, the rotation of the polarisation axis will generally cancel out during one complete roundtrip [25, 26]. However, a linear cavity can still be used for axion frequencies for which the accumulated effect on the laser field also switches sign after half a roundtrip.

Figure 2 assumes the parameters from table 1 and shows the resulting design sensitivity for a shot-noise limited performance at a wavelength of 1064 nm, which is well-known from the gravitational-wave detectors [33, 34]. Hence, $|P_{\mathrm{N}}|^2 = 2\hbar\omega_0 P_{\mathrm{LO}}\sqrt{\tau_a/T_{\mathrm{meas}}}$ in equation (6) with the optical angular frequency ω_0 and the optical power P_{LO} of the local oscillator field. The plotted sensitivity corresponds to the 95% confidence level which is obtained for SNR = 2 in equation (6). DarkGEO-I could already probe a yet unexplored region of the axion-photon parameter space around 1 neV, or 240 kHz, which is favoured by observations of the cosmic infrared background [42].

Please note that we assume a shot-noise limited sensitivity in the whole measurement band. This is an ambitious goal, especially below frequencies of $\sim$1 Hz. However, optical gyroscopes have already demonstrated near-shot-noise limited sensitivities below 1 Hz [43]. Since their operational principle is similar to the one presented here, including common-mode suppressions of displacement noises in the cavity, the assumption of a similar noise budget is realistic. In a more advanced phase of the DarkGEO design, a more thorough model will also include the expected couplings of additional noise source, like

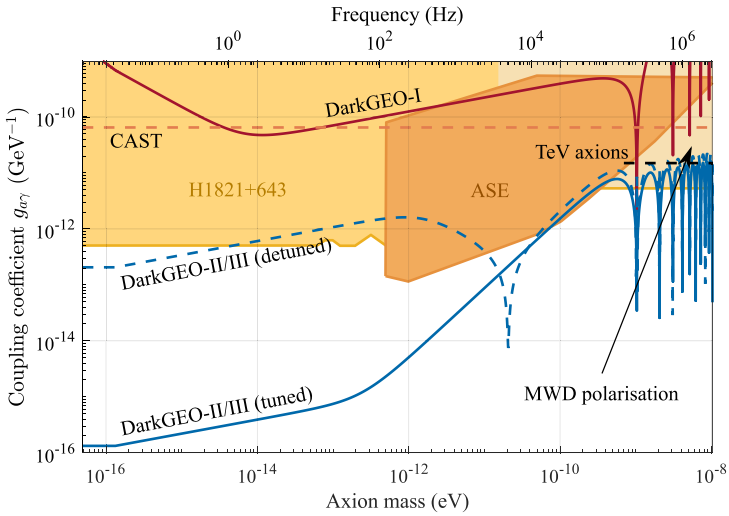

Figure 2. Shot-noise limited design sensitivities at the 95% confidence level to the axion-photon coupling coefficient $g_{a\gamma}$ for DarkGEO-I and -II/-III based on the parameters in table 1. The sensitivities are compared to the CAST limit [20] as well as to the most stringent constraints from astrophysical observations (quasar H1821+643 [39], axion star explosions (ASE) [40], magnetic white dwarf (MWD) polarisation [41]), and to predictions based on the cosmic infrared background ('TeV axions') [42]. 'Tuned' refers to a detuning frequency of $\Delta f = 0$. The 'detuned' case is shown as one example and corresponds to a detuning frequency of $\Delta f = 5\,\mathrm{kHz}$ between the polarisation resonances in the rectangular cavity ($\beta \approx 0.13$).

Table 1. Design parameters for the DarkGEO configurations I and II/III which the sensitivities in figure 2 are based on. The parameters $T_{\mathrm{in/out}}$ refer to the labels in figure 1. For the configuration II/III, 'm' and 'sig' refer to the main laser and signal field, respectively.

Parameter (DarkGEO-I)	Value	Unit
Wavelength	1064	nm
Cavity roundtrip length	1.2	km
Input coupler transmissivity, T_{in}	20	ppm
Output coupler transmissivity, T_{out}	1	ppm
Cavity roundtrip loss, l_{rt}	20	ppm
Laser input power	210	W
Intra-cavity power, $P_{\mathrm{m,cav}}$	10	MW
Measurement time, T_{meas}	1	year
Main laser field polarisation	vertical	
Signal field polarisation	horizontal	
Parameter (DarkGEO-II/III)	**Value**	**Unit**
Wavelength	1064	nm
Cavity roundtrip length	1.2	km
Input coupler transmissivity, $T_{\mathrm{m,in}}$	45	ppm
Output coupler transmissivity, $T_{\mathrm{m,out}}$	1	ppb
Input coupler transmissivity, $T_{\mathrm{sig,in}}$	3000	ppm
Output coupler transmissivity, $T_{\mathrm{sig,out}}$	2.5	ppm
Cavity roundtrip loss, l_{rt}	45	ppm
Laser input power	460	W
Intra-cavity power, $P_{\mathrm{m,cav}}$	10	MW
Effective squeezing level	10	dB
Measurement time, T_{meas}	1	year
Detuning, β	0.13 (scanned)	
Main laser field polarisation	vertical	
Signal field polarisation	horizontal	

technical laser noise and scattered light, to the signal readout as well as means to mitigate them. These means will include e.g. the mode cleaners and a laser power stabilisation, using the fraction of the main laser field that is filtered out in the readout path, against laser intensity noise as well as baffles and mechanical damping against scattered light (compare with [33]). The same holds for the DarkGEO-II/III configuration.

The unprecedented intra-cavity power in the circulating main laser field of 10 MW was assumed as a trade-off between a higher sensitivity and expected practical limits. This power was also chosen as a target for selecting the design parameters in table 1. This target will be achieved by operating the cavity in the

over-coupled impedance regime and reading out the signal in reflection. The input and output coupler transmissivities of 20 ppm and 1 ppm, respectively, were chosen to yield a high power buildup factor of about 47 500 assuming a roundtrip power loss of 20 ppm. This allows for a power of 10 MW in combination with an already existing laser source which provides about 210 W [44]. Furthermore, an optical power of 10 MW on the GEO600 mirrors corresponds to a similar optical intensity as already reached in LIDA (4.7 MW cm^{-2}) since beam sizes of up to a few centimetres will be possible in DarkGEO.

It is important to note that if any of these design parameters (especially the high intra-cavity power) should not be exactly met, this would only result in a corresponding slight reduction in the design sensitivity, and DarkGEO could still significantly surpass the current constraints of axion searches.

The input and output mode cleaners filter out technical laser noise above their pole frequencies as well as unwanted higher-order spatial modes. The local oscillator field for the readout can be obtained by rotating the polarising beamsplitter, accordingly.

3.2. DarkGEO-II: rectangular configuration

DarkGEO-II assumes the LIDA design with a rectangular cavity and requires larger changes to the GEO600 facility in order to set up pairs of mirrors on either side of the 600 m long vacuum tube. The laser input and signal readout will, however, remain the same as in DarkGEO-I. This is also shown in figure 1 (bottom schematic). As before, we propose a readout in reflection of the cavity to reach a circulating power of 10 MW in the main laser field, despite an assumed roundtrip loss of 45 ppm, by operating the cavity in the over-coupled impedance regime. In this configuration, the design parameters yield a cavity power buildup factor of about 22 000 such that the laser source has to provide 460 W. While this level has not been reached yet by a single-frequency, low-noise laser, this goal is in line with the current research in the gravitational-wave community: the Einstein Telescope plans to utilise a 500 W laser source [45], and up to 370 W in the fundamental Gaussian laser mode have already been achieved [44]. Hence, the development of a sufficiently strong laser source by the time DarkGEO-II could be initiated is a realistic assumption.

In the rectangular configuration, the signal field experiences higher input and output coupler transmissivities than the main laser field if the signal field's axis of polarisation is chosen to be horizontal. Given the parameters from table 1, the cavity's power reflection coefficient for the signal field's polarisation at the resonance condition becomes about 94%, causing only little optical loss to a field between the cavity's input and reflection port. Hence, we propose the injection of squeezed states of light in the signal field's polarisation (horizontal), as shown in figure 1, to mitigate quantum shot noise. Here, shot noise is mainly caused by the vacuum fluctuations that enter the cavity from the laser input side in the polarisation of the signal field, are effectively reflected and reach the signal readout. These vacuum fluctuations are replaced by squeezed vacuum as already done in a similar way in the gravitational-wave detectors GEO600, Advanced LIGO and Advanced Virgo [38, 46, 47]. We assume the same ambitious squeezing level of 10 dB as envisaged for the next-generation gravitational-wave detectors, the Einstein Telescope [45] and Cosmic Explorer [48], and as, so far, only achieved in tabletop experiments [49, 50]. The squeezing level is included as a factor of e^{-2r} in $|P_{\mathrm{N}}|^2$ in equation (6).

An additional aspect of the rectangular cavity is that the mirrors distinguish between vertical (main laser field) and horizontal (signal field) linear polarisation. This especially holds for the phases which the two polarisations accumulate during one cavity roundtrip. Hence, their resonances are not necessarily degenerate in frequency which affects the detector's sensitivity curve with respect to the axion field's frequency. Let's assume the cavity resonances for vertical and horizontal polarisation are detuned by Δf (detuning frequency). Since an axion field excites two signal sidebands which are shifted in frequency relative to the main laser field by $\pm\Omega_a$, any sideband is strongly amplified by the resonant power buildup inside the cavity if $\pm\Omega_a$ is sufficiently close to Δf. Hence, the detector will have its primary sensitivity peak at the frequency Δf. Controlling the detuning frequency, e.g. via an auxiliary cavity as proposed in [25], would thus allow to control at which frequency, or axion mass, the detector reaches its peak sensitivity.

Figure 2 shows the shot-noise limited sensitivities that DarkGEO-II could reach with the parameters given in table 1. The chosen example for the 'detuned' case ($\Delta f \neq 0$) indicates how a scan of the frequency detuning will scan the most prominent sensitivity peak through the spectrum. DarkGEO-II could significantly surpass the most stringent constraints of the axion-photon coupling in almost its entire measurement band from 10^{-16} to 10^{-8}eV.

This fact impressively highlights the motivation and importance for upscaling the LIDA detector in the GEO600 facilities. While the general optical setup is the same for LIDA and DarkGEO, the increase of the physical length by two orders of magnitude and the increase of the maximum intra-cavity power by another two orders of magnitude result in a DarkGEO sensitivity which surpasses even the most optimistic LIDA projections by about three orders of magnitude. Hence, DarkGEO is essential to reach below the constraints set by astrophysical observations.

3.3. DarkGEO-III: full coincidence search

For the final iteration step, a second rectangular cavity is set up in the second vacuum tube of the GEO600 facilities. Hence, DarkGEO-III will operate two identical and, more importantly, independent axion detectors at the same time, which are influenced by an axion field in the same way. The disadvantage of the LIDA and DANCE design is that these detectors cannot be operated in a state where they are insensitive to axions. It is, thus, non-trivial to determine whether a potential signature is real or caused by noise. The operation of two independent detectors, however, allows to search for coincident signals which are significantly less likely to be caused by the uncorrelated noise sources of the two detectors.

Please note that a true independence between the two detectors is a challenge on its own since they will share the central vacuum chamber. In an advanced phase of the DarkGEO design, means to mitigate any possible cross-talk have to be specified.

4. Challenges

4.1. Non-planarity in DarkGEO-II/III

LIDA has observed a cross-talk between vertically and horizontally polarised light inside the optical cavity [31]. When injecting a vertically polarised laser beam into the cavity, the authors obtained an elliptically polarised laser beam in transmission which only consisted of the injected vertical polarisation to 82%–85%. This observation can partly be explained by a non-planarity of the rectangular cavity, leading to a coupling of the external orthogonal states of polarisation.

We modelled this effect using an ABCDEF matrix beam propagation method to compute an estimate for this coupling in DarkGEO-II and -III. In this model, the cavity has the dimensions of $L \times l = 600\,\mathrm{m} \times 40\,\mathrm{cm}$ to fit into the 60 cm wide vacuum tubes of the GEO600 facilities. Given the current GEO600 mirrors with a diameter of 18 cm, we assume a beam waist of about 2.2 cm and a radius of curvature on one of the mirrors of $R_c = 3000\,\mathrm{m}$. The matrix for the free space propagation $V_{L(l)}$ along the length of $L\,(l)$ and the matrix for the reflection off the four mirrors M are given by

$$V_{L(l)} = \begin{pmatrix} 1 & L\,(l) & 0 \\ 0 & 1 & 0 \\ 0 & 0 & 1 \end{pmatrix}, M_k = \begin{pmatrix} 1 & 0 & 0 \\ 0 & \left(-\frac{2}{R_c}\right) & 1 & 2\alpha_k \\ 0 & 0 & 1 \end{pmatrix} \tag{7}$$

where $k = 1, 2, 3, 4$ are the four mirrors and α_k are their misalignments. Further, the terms in brackets are not factors but the matrix elements for the propagation along l and for the reflection off the curved mirror, respectively. The upper limit for the mirror misalignment, causing the non-planarity, is set to 75 μrad, which corresponds to a displacement of the beam by half of a mirror radius over a distance of 600 m. Finally, the eigenvalue problem of the cavity matrix

$$C = M_1\, V_l M_4\, V_L\, M_3\, V_l M_2\, V_L \tag{8}$$

is solved for the power ratio between the light in the vertical and horizontal polarisation in transmission of the cavity.

If a purely vertically polarised field is injected, figure 3 shows that the coupling of the horizontal polarisation into the transmitted field remains below 1%, even for a misalignment >75 μrad. Hence, DarkGEO should already strongly mitigate this effect via its physical size.

4.2. Drifts of the frequency separation

As mentioned in section 3.2, the cavity resonances of the main laser field's and signal field's polarisation are likely to be separated in frequency in DarkGEO-II and -III (detuning). While there are means to control and stabilise this detuning [25], an estimation of how much a free-running detuning may drift during operation is important, as well. We have conducted a test run with LIDA where we have tracked the detuning over a time of 141 h.

If the polarisation of the input field is slightly rotated relative to either the horizontal or vertical polarisation, this input field partially couples to the respective orthogonal polarisation, as well. Most importantly, the technical noise of this fraction of the input field will then be transmitted through the cavity around the detuning frequency. Hence, we obtain a prominent noise peak in the readout spectrum whose frequency coincides with the detuning frequency and which can be tracked over time.

For this test run, we chose the linear polarisation of the input field to be mainly horizontal, associated with a significantly lower finesse than the vertical polarisation. This allowed for a more reliable long-term operation and resulted in a narrower, more defined peak in the readout spectrum which now corresponded

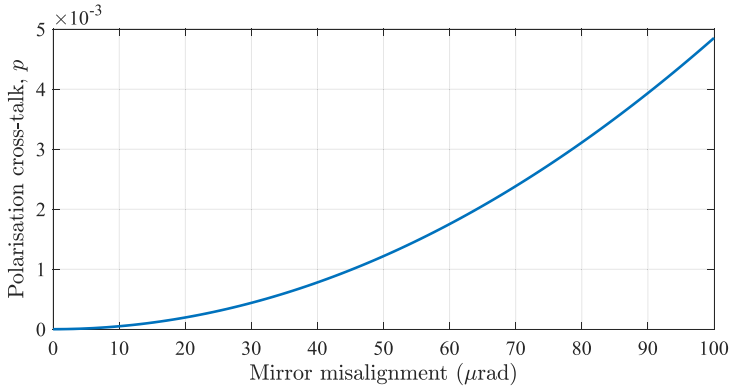

Figure 3. Cross-talk between the external vertical and horizontal states of linear polarisation in the rectangular cavities of DarkGEO-II and -III. Assuming that a pure vertically polarised field is injected, p indicates the contribution of the horizontal polarisation to the transmitted field due to a mirror misalignment and due to the resulting cavity non-planarity.

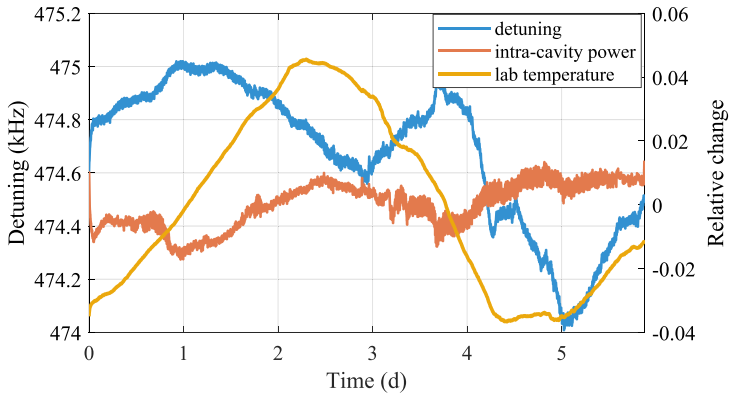

Figure 4. Evolution of the frequency separation between the cavity resonances of the horizontal and vertical linear polarisation (detuning) during a test run of 141 h (left y-axis, starting at about 474.8 kHz). The full range of the detuning drift was about 1 kHz, or 0.2%. The evolutions of the circulating intra-cavity power and of the lab temperature (right y-axis, ending at about 0.01 and −0.01, respectively) do not show an obvious correlation over the full measurement time.

to the higher finesse of the vertical polarisation. The circulating intra-cavity power was about 580 W (intensity of 22 kW cm^{-2} at the waist).

As figure 4 shows, the detuning only drifted over a range of about 1 kHz, which amounts to 0.2% of the mean detuning of 474.5 kHz. Figure 4 also compares the evolution of this detuning to the evolution of the lab temperature and of the circulating intra-cavity power in terms of their change relative to their respective mean value. This comparison was used to infer whether thermo-optic changes in the mirror substrates and coatings due to the residual absorption of the circulating laser power or changes in the ambient temperature are the underlying cause of the drift of the detuning. While there occasionally seems to be a correlation to the intra-cavity power over the first 4.5 days, the detuning especially shows a rather sharp dip over the last day even though the power is roughly constant. There also seems to be a correlation to the lab temperature over the last half of the time with a delay of 1–2 days (and no delay from day 5). However, the first peak in the detuning does not have a counterpart in the evolution of the lab temperature. Thus, there is no obvious correlation of the detuning to either the intra-cavity power or the lab temperature which persists over the full measurement time.

Hence, we have not conclusively found a mechanism behind the drift of the detuning frequency. Still, we could confirm that the detuning frequency was quite stable and only drifted within a range that is a factor of 13.5 smaller than LIDA's measurement bandwidth (see the parameter $f_{\mathrm{p,P}}$ in [31]). While we aim to further investigate the cause of this drift, especially at higher levels of optical power, the potential implementation of an auxiliary cavity, or any other means to control the detuning frequency, should be part of the reconstruction plans for the GEO600 facilities towards DarkGEO-II and -III. A drift of about ±500 Hz was not critical for LIDA's first observing run because the mean detuning was three orders of magnitude larger and the measurement bandwidth was more than one order of magnitude larger as well. However, the same drift could reduce the sensitivity of the tuned DarkGEO-II and -III case (see figure 2) by 1 to 2 orders

magnitude below 100 Hz since the mean detuning is targeted to be zero. The theory of controlling the detuning frequency with an auxiliary cavity is straightforward and already further investigated for the DANCE detector [25, 51].

4.3. Thermal effects

At the high operating optical intensity, LIDA experienced occasional drops in the intra-cavity power in a range from 10% up to 50% correlated with an increase in the readout noise as well as a deterioration of the output beam purity [31]. Even though this effect is not fully understood yet, it is likely to be related to parametric instabilities (PIs) [52]. A PI occurs when the main spatial laser mode which resonates in a cavity, here the fundamental Gaussian TEM_{00} mode, couples to an excited vibrational eigenmode of a mirror. This interaction leads to light being scattered into a higher-order transverse laser mode. In addition, thermal deformations of the mirror surfaces caused by the absorption of the high circulating laser power may affect the cavity's transverse mode spacing and, thus, result in a co-resonance of the TEM_{00} and a higher-order mode. If this co-resonating higher-order mode is also coupled to the TEM_{00} mode via the PI, this mechanism could explain the observed thermal effect in LIDA.

If this mechanism is confirmed after additional investigation, we propose to use acoustic mode dampers to significantly reduce the quality factors of the mirror's vibrational eigenmodes [53]. The risk of increasing thermal noise by adding this channel of energy dissipation does not apply to the discussed laser-interferometric axion detectors as the main laser field and signal field are co-propagating and, thus, any common mode effect cancels out [25]. Still, a more detailed future model might need to include thermally induced effects as well, e.g. regarding birefringence that converts the vertical to the horizontal polarisation or vice versa.

5. Conclusion

The gravitational-wave detector and technology testbed GEO600 in Germany provides an excellent facility to house a kilometre-scale laser-interferometric axion detector, DarkGEO. We showed how such a transformation could be executed in a 3-step programme. In the first step, DarkGEO-I will operate a linear cavity to search for axions and axion-like particles around the free-spectral ranges. DarkGEO-II will then operate a rectangular cavity based on the LIDA topology, and DarkGEO-III will finally consist of two such independent detectors for a coincident search. The presented design parameters allow for sensitivities to the axion-photon coupling coefficient that are several orders of magnitude below the current most stringent constraints within a mass range of 10^{-16} to 10^{-8}eV. DarkGEO would, thus, be an immense and vital advance of direct axion searches. In addition, DarkGEO would still serve as a technology demonstrator for the third generation of gravitational-wave detectors, the Einstein Telescope and Cosmic Explorer. This especially applies to the envisaged high-power laser source, the unprecedented intra-cavity power and the effective squeezing level of 10 dB in a complex, large-scale experiment. Moreover, we discussed the main challenges which are known from the first LIDA results: cross-talk between the horizontal and vertical polarisation, drifts of the detuning frequency and thermal effects inside the optical cavity. The proposed solutions should significantly limit the impact of these effects to enable a robust long-term operation at the simulated design sensitivities.

Data availability statement

The data that support the findings of this study are available upon reasonable request from the authors.

Acknowledgments

We acknowledge members of the UK Quantum Interferometry collaboration for useful discussions, the support of the Institute for Gravitational Wave Astronomy at the University of Birmingham and STFC Quantum Technology for Fundamental Physics scheme (Grant Nos. ST/T006331/1, ST/T006609/1 and ST/W006375/1). D M is supported by the 2021 Philip Leverhulme Prize.

ORCID iDs

Joscha Heinze https://orcid.org/0000-0001-8692-2724
Alex Gill https://orcid.org/0009-0008-9084-6857
Artemiy Dmitriev https://orcid.org/0000-0002-0314-956X
Jiří Smetana https://orcid.org/0000-0002-7277-6671

Tianliang Yan https://orcid.org/0000-0002-2639-1500
Vincent Boyer https://orcid.org/0000-0002-6900-8786
Denis Martynov https://orcid.org/0000-0003-0679-1344
Hartmut Grote https://orcid.org/0000-0002-0797-3943
James Lough https://orcid.org/0000-0002-5160-0239
Aldo Ejlli https://orcid.org/0000-0002-4149-4532
Guido Müller https://orcid.org/0000-0003-2262-4132

References

[1] Akerib D *et al* 2013 The Large Underground Xenon (LUX) experiment *Nucl. Instrum. Methods Phys. Res.* A **704** 111–26
[2] Aprile E *et al* 2018 Dark matter search results from a one ton-year exposure of XENON1T *Phys. Rev. Lett.* **121** 111302
[3] Zhang H *et al* 2018 Dark matter direct search sensitivity of the PandaX-4T experiment *Sci. China Phys. Mech. Astron.* **62** 31011
[4] Abbott L and Sikivie P 1983 A cosmological bound on the invisible axion *Phys. Lett.* B **120** 133–6
[5] Preskill J, Wise M B and Wilczek F 1983 Cosmology of the invisible axion *Phys. Lett.* B **120** 127–32
[6] Dine M and Fischler W 1983 The not-so-harmless axion *Phys. Lett.* B **120** 137–41
[7] Peccei R D and Quinn H R 1977 CP conservation in the presence of pseudoparticles *Phys. Rev. Lett.* **38** 1440–3
[8] Weinberg S 1978 A new light boson? *Phys. Rev. Lett.* **40** 223–6
[9] Wilczek F 1978 Problem of strong *P* and *T* invariance in the presence of instantons *Phys. Rev. Lett.* **40** 279–82
[10] Chadha-Day F, Ellis J and Marsh D J E 2022 Axion dark matter: what is it and why now? *Sci. Adv.* **8** eabj3618
[11] Svrcek P and Witten E 2006 Axions in string theory *J. High Energy Phys.* JHEP06(2006)051
[12] Graham P W and Rajendran S 2013 New observables for direct detection of axion dark matter *Phys. Rev.* D **88** 035023
[13] Ringwald A 2012 Exploring the role of axions and other WISPs in the dark Universe *Phys. Dark Universe* **1** 116–35
[14] Ringwald A 2014 Searching for axions and ALPs from string theory *J. Phys.: Conf. Ser.* **485** 012013
[15] Farina M, Pappadopulo D, Rompineve F and Tesi A 2017 The photo-philic QCD axion *J. High Energy Phys.* JHEP01(2017)095
[16] Amruth A *et al* 2023 Einstein rings modulated by wavelike dark matter from anomalies in gravitationally lensed *Nat. Astron.* **7** 736–47
[17] Bartram C *et al* 2021 Search for invisible axion dark matter in the 3.3–4.2 eV mass range *Phys. Rev. Lett.* **127** 261803
[18] Caldwell A, Dvali G, Majorovits B, Millar A, Raffelt G, Redondo J, Reimann O, Simon F and Steffen F (MADMAX Working Group) 2017 Dielectric haloscopes: a new way to detect axion dark matter *Phys. Rev. Lett.* **118** 091801
[19] Brouwer L *et al* 2022 Projected sensitivity of DMRadio-m^3: a search for the QCD axion below 1 μeV *Phys. Rev.* D **106** 103008
[20] Anastassopoulos V *et al* (CAST) 2017 New CAST limit on the axion-photon interaction *Nat. Phys.* **13** 584–90
[21] Armengaud E *et al* 2014 Conceptual design of the international axion observatory (IAXO) *JINST J. Instrum.* **9** T05002
[22] Bähre R *et al* 2013 Any light particle search II—technical design report *J. Instrum.* **8** T09001
[23] Betz M, Caspers F, Gasior M, Thumm M and Rieger S W 2013 First results of the CERN resonant weakly interacting sub-eV particle search (CROWS) *Phys. Rev.* D **88** 075014
[24] Salemi C P *et al* 2021 Search for low-mass axion dark matter with ABRACADABRA-10 cm *Phys. Rev. Lett.* **127** 081801
[25] Martynov D and Miao H 2020 Quantum-enhanced interferometry for axion searches *Phys. Rev.* D **101** 095034
[26] DeRocco W and Hook A 2018 Axion interferometry *Phys. Rev.* D **98** 035021
[27] Obata I, Fujita T and Michimura Y 2018 Optical ring cavity search for axion dark matter *Phys. Rev. Lett.* **121** 161301
[28] Liu H, Elwood B D, Evans M and Thaler J 2019 Searching for axion dark matter with birefringent cavities *Phys. Rev.* D **100** 023548
[29] Michimura Y, Oshima Y, Watanabe T, Kawasaki T, Takeda H, Ando M, Nagano K, Obata I and Fujita T 2020 DANCE: dark matter axion search with riNg cavity experiment *J. Phys.: Conf. Ser.* **1468** 012032
[30] Nagano K, Fujita T, Michimura Y and Obata I 2019 Axion dark matter search with interferometric gravitational wave detectors *Phys. Rev. Lett.* **123** 111301
[31] Heinze J, Gill A, Dmitriev A, Smetana J, Yan T, Boyer V, Martynov D and Evans M 2024 First results of the Laser-Interferometric Detector for Axions (LIDA) *Phys. Rev. Lett.* **132** 191002
[32] Oshima Y, Fujimoto H, Kume J, Morisaki S, Nagano K, Fujita T, Obata I, Nishizawa A, Michimura Y and Ando M 2023 First results of axion dark matter search with DANCE *Phys. Rev.* D **108** 072005
[33] Buikema A *et al* 2020 Sensitivity and performance of the advanced LIGO detectors in the third observing run *Phys. Rev.* D **102** 062003
[34] Bersanetti D, Patricelli B, Piccinni O J, Piergiovanni F, Salemi F and Sequino V 2021 Advanced Virgo: status of the detector, latest results and future prospects *Universe* **7** 322
[35] Collaboration KAGRA 2022 Performance of the KAGRA detector during the first joint observation with GEO600 (O3GK) *Prog. Theor. Exp. Phys.* **2023** 10A101
[36] Budker D, Graham P W, Ledbetter M, Rajendran S and Sushkov A O 2014 Proposal for a cosmic axion spin precession experiment (CASPEr) *Phys. Rev.* X **4** 021030
[37] de Salas P F and Widmark A 2021 Dark matter local density determination: recent observations and future prospects *Rep. Prog. Phys.* **84** 104901
[38] Lough J *et al* 2021 First demonstration of 6 dB quantum noise reduction in a kilometer scale gravitational wave observatory *Phys. Rev. Lett.* **126** 041102
[39] Sisk-Reynés J, Matthews J H, Reynolds C S, Russell H R, Smith R N and Marsh M C D 2021 New constraints on light axion-like particles using Chandra transmission grating spectroscopy of the powerful cluster-hosted quasar H1821+643 *Mon. Not. R. Astron. Soc.* **510** 1264–77
[40] Escudero M, Pooni C K, Fairbairn M, Blas D, Du X and Marsh D J E 2024 Axion star explosions: a new source for axion indirect detection *Phys. Rev.* D **109** 043018
[41] Dessert C, Dunsky D and Safdi B R 2022 Upper limit on the axion-photon coupling from magnetic white dwarf polarization *Phys. Rev.* D **105** 103034
[42] Kohri K and Kodama H 2017 Axion-like particles and recent observations of the cosmic infrared background radiation *Phys. Rev.* D **96** 051701

[43] Schreiber K U, Klügel T, Wells J P R, Hurst R B and Gebauer A 2011 How to detect the chandler and the annual wobble of the earth with a large ring laser gyroscope *Phys. Rev. Lett.* **107** 173904
[44] Wellmann F, Bode N, Wessels P, Overmeyer L, Neumann J, Willke B and Kracht D 2021 Low noise 400 W coherently combined single frequency laser beam for next generation gravitational wave detectors *Opt. Express* **29** 10140–9
[45] ET Steering Committee 2020 ET design report update (available at: www.et-gw.eu/index.php/relevant-et-documents) (Accessed 2 April 2022)
[46] The LIGO Scientific Collaboration 2013 Enhanced sensitivity of the LIGO gravitational wave detector by using squeezed states of light *Nat. Photon.* **7** 613–9
[47] Acernese F *et al* 2019 Increasing the astrophysical reach of the Advanced Virgo detector via the application of squeezed vacuum states of light *Phys. Rev. Lett.* **123** 231108
[48] Evans M *et al* 2021 A horizon study for cosmic explorer: science, observatories, and community (arXiv:2109.09882)
[49] Heinze J, Danzmann K, Willke B and Vahlbruch H 2022 10 dB quantum-enhanced Michelson interferometer with balanced homodyne detection *Phys. Rev. Lett.* **129** 031101
[50] Zander J, Rembe C and Schnabel R 2022 10 dB interferometer enhancement by squeezing of photon shot noise with sub-femtometer resolution and eye-safe optical power *Quantum Sci. Technol.* **8** 01LT01
[51] Fujimoto H, Oshima Y, Ando M, Fujita T, Michimura Y, Nagano K and Obata I 2021 Dark matter axion search with riNg cavity experiment DANCE: design and development of auxiliary cavity for simultaneous resonance of linear polarizations *J. Phys.: Conf. Ser.* **2156** 012182
[52] Evans M, Barsotti L and Fritschel P 2010 A general approach to optomechanical parametric instabilities *Phys. Lett.* A **374** 665–71
[53] Biscans S, Gras S, Blair C D, Driggers J, Evans M, Fritschel P, Hardwick T and Mansell G 2019 Suppressing parametric instabilities in LIGO using low-noise acoustic mode dampers *Phys. Rev.* D **100** 122003